ACTA NEUROBIOLOGIAE EXPERIMENTALIS

Research paper Acta Neurobiol Exp 2012, 72: 79–87

Object-based analysis of astroglial reaction and astrocyte subtype morphology after ischemic brain injury

Daniel-Christoph Wagner[1,2]*, Johanna Scheibe[1], Isabelle Glocke[1], Gesa Weise[1,2], Alexander Deten[1,2], Johannes Boltze[1,2,3], and Alexander Kranz[1,2]

[1]Fraunhofer Institute for Cell Therapy and Immunology, Leipzig, Germany; [2]Translational Center for Regenerative Medicine, Leipzig, Germany, *Email: daniel-christoph.wagner@izi.fraunhofer.de; [3]Massachusetts General Hospital and Harvard Medical School, Boston, MA, USA

The astrocytic response to ischemic brain injury is characterized by specific alterations of glial cell morphology and function. Various studies described both beneficial and detrimental aspects of activated astrocytes, suggesting the existence of different subtypes. We investigated this issue using a novel object-based approach to study characteristics of astrogliosis after stroke. Spontaneously hypertensive rats received permanent middle cerebral artery occlusion. After 96 h, brain specimens were removed, fixed and stained for GFAP, glutamine synthetase (GS), S100β and Musashi1 (Msh1). Three regions of interest were defined (contralateral hemisphere, ipsilateral remote zone and infarct border zone), and confocal stacks were acquired (n=5 biological with each n=4 technical replicates). The stacks were background-corrected and colocalization between the selected markers and GFAP was determined using an automated thresholding algorithm. The fluorescence and colocalization channels were then converted into 3D-objects using both intensity and volume as filters to ultimately determine the final volumes of marker expression and colocalization, as well as the morphological changes of astrocyte process arborisation. We found that both S100β and Msh1 determined the same GFAP-positive astroglial cell population albeit the cellular compartments differed. GFAP stained most of the astrocyte processes and is hence suitable for the analysis of qualitative characteristics of astrogliosis. Due to its peri-nuclear localization, Msh1 is appropriate to estimate the total number of astrocytes even in regions with severe reactive astrogliosis. GS expression in GFAP-positive astrocytes was high in the remote zone and low at the infarct border, indicating the existence of astrocyte subclasses.

Key word: astrocytes, reactive astrogliosis, immunohistochemistry, brain ischemia, confocal microscopy

INTRODUCTION

Reactive astrogliosis following brain damage is characterized by specific alterations of astrocyte phenotype and function. This response can be roughly categorized into two major patterns (Sofroniew and Vinters 2010). In the context of brain inflammation, or remote from focal lesions, astrocytes show mild to moderate responses characterized by hypertrophy of cell soma and processes and an upregulation of intermediary filaments, but preserved individual domains (Wilhelmsson et al. 2006). The impact of those changes is not fully understood, but they may be associated with pro-regenerative properties (Liberto et al. 2004). In regions of serious brain damage, reactive astrogliosis is additionally characterized by interlacing processes, cellular proliferation and the disruption of individual domains. Genetic ablation of reactive astrocytes showed that the latter process is vital for the restriction of the adverse inflammatory environment present after spinal cord injury, stroke and other causes of central nervous system damage (Okada et al. 2006, Sofroniew and Vinters 2010, Shimada et al. 2011). In contrast, the chronic sequelae of glial scarring imply a regenerative failure owing to an inhibiting environment for axonal and synaptic plasticity (Menet et al. 2003, Silver and Miller 2004). Hence, reactive astrogliosis may have ambivalent effects depending on where and when it occurs.

Correspondence should be addressed to D.C. Wagner
Email: daniel-christoph.wagner@izi.fraunhofer.de

Received 15 December 2012, accepted 05 February 2013

It is, however, not fully elucidated if the putative entity of reactive astrocytes can be differentiated into functionally distinct subclasses and how these could be identified. This persistent problem of astrocyte identity (Kimelberg 2004) is mainly due to the fact that the expression of astrocyte markers depends on species, age, anatomical location and several other variables. Heterogeneity of astrocytes has repeatedly been described, mostly by means of different immunohistochemical markers (Wang and Walz 2003, Oki et al. 2010, White et al. 2010) but also by quantification of individual cell volumes in GFAP/eGFP mice (Benesova et al. 2009), by measuring ionic currents (Walz 2000) or by primary cell gene expression analysis (Stahlberg et al. 2011). The immunohistochemical detection and colocalization of different markers *in situ* might be particularly appropriate to study astrogliosis, since it has been shown that reactive astrocytes recapitulate embryonic markers such as nestin (Takahashi et al. 2007, Popa-Wagner et al. 2011) and Musashi1 (Oki et al. 2010) and may change their marker expression as surrogate of a functional adjustment (Wang et al. 2004, Zou et al. 2011). Thus, functional subclasses of astrocytes can be discriminated by investigating the co-expression of distinct markers.

Quantitative colocalization analysis in CNS tissue, on the other hand, is confounded by numerous technical problems. Most studies assess colocalization solely by visual inspection and therefore obtain only a binarized picture of overlap (e.g. the cell is either negative or positive for one marker). Such pictures, however, do not account for the fact that the overall degree of colocalization may differ, and that colocalization may occur and change in different compartments of the astrocyte. Furthermore, established procedures for quantitative assessment of colocalization, such as Pearson's Correlation Coefficient and Mander's Colocalization Coefficient are highly sensitive for background noise and non-linear colocalization scenarios (Bolte and Cordelieres 2006, Comeau et al. 2006, Singan et al. 2011). This limitation frequently applies to immunohistochemically stained brain sections particularly after injury, which commonly causes an increase of tissue autofluorescence. This might explain why quantitative colocalization analyses of reactive astrocytes in damaged brain specimens have, to our knowledge, not been described yet.

In the present study, we used an object-based approach to overcome the limitations of existing colocalization measures (Bolte and Cordelieres 2006) to ultimately investigate and quantify the co-expression of different astrocyte markers. For this, we combined automated colocalization analysis with an object segmentation approach that uses both intensity and object volume to exclude noise. A further advantage of this three-dimensional approach is that it can also be used to determine certain phenotypic characteristics of the astrocyte processes.

METHODS

Experimental cerebral ischemia and tissue sampling

Animal procedures were carried out according to the Guide for the Care and Use of Laboratory Animals published by the US National Institutes of Health (NIH Publication No. 85-23, revised 1996), and approved by the appropriate federal agency (reference number TVV18/07). Five male spontaneously hypertensive rats (Charles River, Sulzfeld, Germany) at the age of 12 weeks were subjected to permanent middle cerebral artery occlusion (pMCAO) as described previously (Riegelsberger et al. 2011). At four days after stroke onset, animals were deeply anesthetized, sacrificed by CO_2 and transcardially perfused with 50 mL body-warm phosphate buffered saline (PBS) followed by 300 mL ice-cold formalin solution (4%). Removed brain specimens were post-fixed in 4% formalin solution, vitrified in 30% sucrose solution and cryoconserved at −80°C. Frozen brains were cut into 40 µm thick free-floating coronal sections and stored in tissue cryoprotectant at −20°C until further use.

Immunohistochemistry

Immunohistochemical staining was performed on cryosections obtained from four distinct brain regions: Bregma anterior-posterior +2.0 mm, +1.5 mm, +1.0 mm and +0.5 mm according to the Paxinos and Watson atlas (2006). Mounted cryosections were first subjected to antigen retrieval for 35 min at 80°C and blocked for non-specific binding using 5% goat serum plus 0.3% Trition-X-100 in PBS for one hour at room temperature. Sections were then incubated with an anti-glial fibrillary acidic protein (GFAP) antibody (rabbit anti-GFAP, 1:200, Sigma-Aldrich or mouse anti-GFAP Alexa Fluor 488 conjugated, 1:200, Millipore) and one

of the following primary antibodies for 24 h at 4°C: mouse anti-Glutamine Synthetase (GS; 1:200, Millipore), rabbit anti-Musashi1 (Msh1, 1:200, Abcam) and mouse anti-S100 calcium binding protein beta (S100β, 1:200, Abcam). Next, the sections were incubated with corresponding fluorochromated secondary antibodies for one hour at room temperature (goat anti-rabbit Alexa Fluor 488, anti-mouse Alexa Fluor 546 and anti-rabbit Alexa Fluor 546, each 1:200, Invitrogen). As negative control, one brain section from each region was processed analogously to the according staining procedure except the use of primary antibodies.

Data recording and image processing

Slices were analyzed by a Zeiss LSM710 (Laser: Diode 405, Argon 488, Helium-Neon 545; objective: Plan-Apochromat 63×/1.40 oil). *Z*-stacks of approximately 15 µm were taken in steps of 0.48 µm. Images of a size of (xy) 135 × 135 µm were acquired with a resolution 512 × 512 pixels, twofold line averaging, and using constant values for laser power, pinhole, digital gain, offset, and scan speed. The detection gains were set to standard values, but corrected where required until few specific pixels (i.e. within cellular structures) reached oversaturation. Files were saved in a compression-free format. On each of the four slices (Bregma anterior-posterior +2.0 mm, +1.5 mm, +1.0 mm and +0.5 mm) image stacks were acquired in three defined brain regions of interest (ROI; Fig. 1): (1) a cortical infarct border zone (IBZ), defined by the middle of the tangent to the cortical lesion, (2) an ipsilateral cortical remote zone (RZ), adjacent to the interhemispheric gap and (3) a control region within the contralateral hemisphere (CH) cortex equivalent to the location of the IBZ.

The acquired image stacks were further processes using the Imaris software (Version 7.4.2, Bitplane, Zurich, Switzerland). After background correction, colocalization between GFAP and the according second channel was assessed by using an automated thresholding algorithm (Costes et al. 2004). The obtained colocalized voxels within one stack, as well as the two initial channels were rendered into three-dimensional objects. The thresholds of the two initial channels were set to the value that has been determined by the automated thresholding during colocalization. According to the assumption that background noise should be small, only objects larger than 30 voxels were included in the object compilation. The vol-

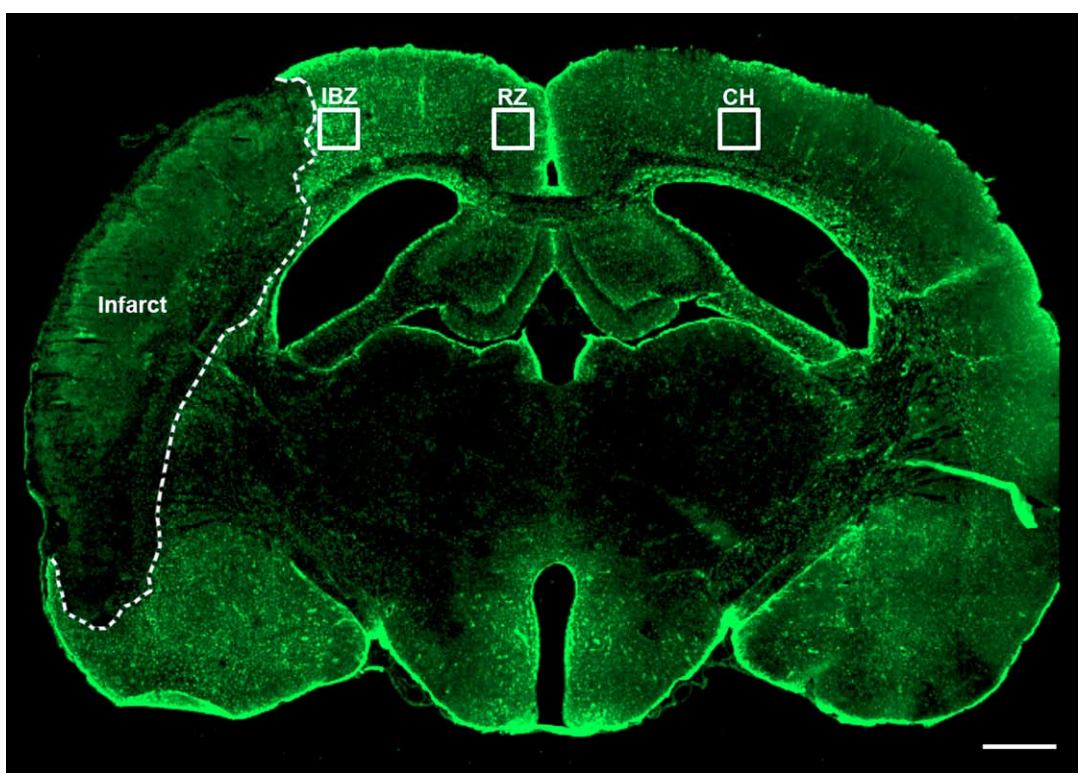

Fig. 1. Representative brain section stained for GFAP showing the regions of interest used for analysis. Scale bar is 1 mm.

ume of the obtained objects was expressed as percentage of the volume of the ROI. Next, we used the FilamentTracer module (Imaris) to quantify morphological changes of astrocyte processes using the following endpoints: mean process diameter, length and branching and the summarized process volume. Finally, we used the objects obtained from the colocalization analysis of GFAP and Msh1 to determine the number of GFAP/Msh1 double-positive astrocytes within the according ROI. The latter investigation was solely performed within the remote zone and the infarct border zone, since the expression of Msh1 in the contralateral control region was mostly below the detection limit.

Statistical data analysis

All data were assessed in technical quadruplicates (four anatomical regions) that were averaged for further

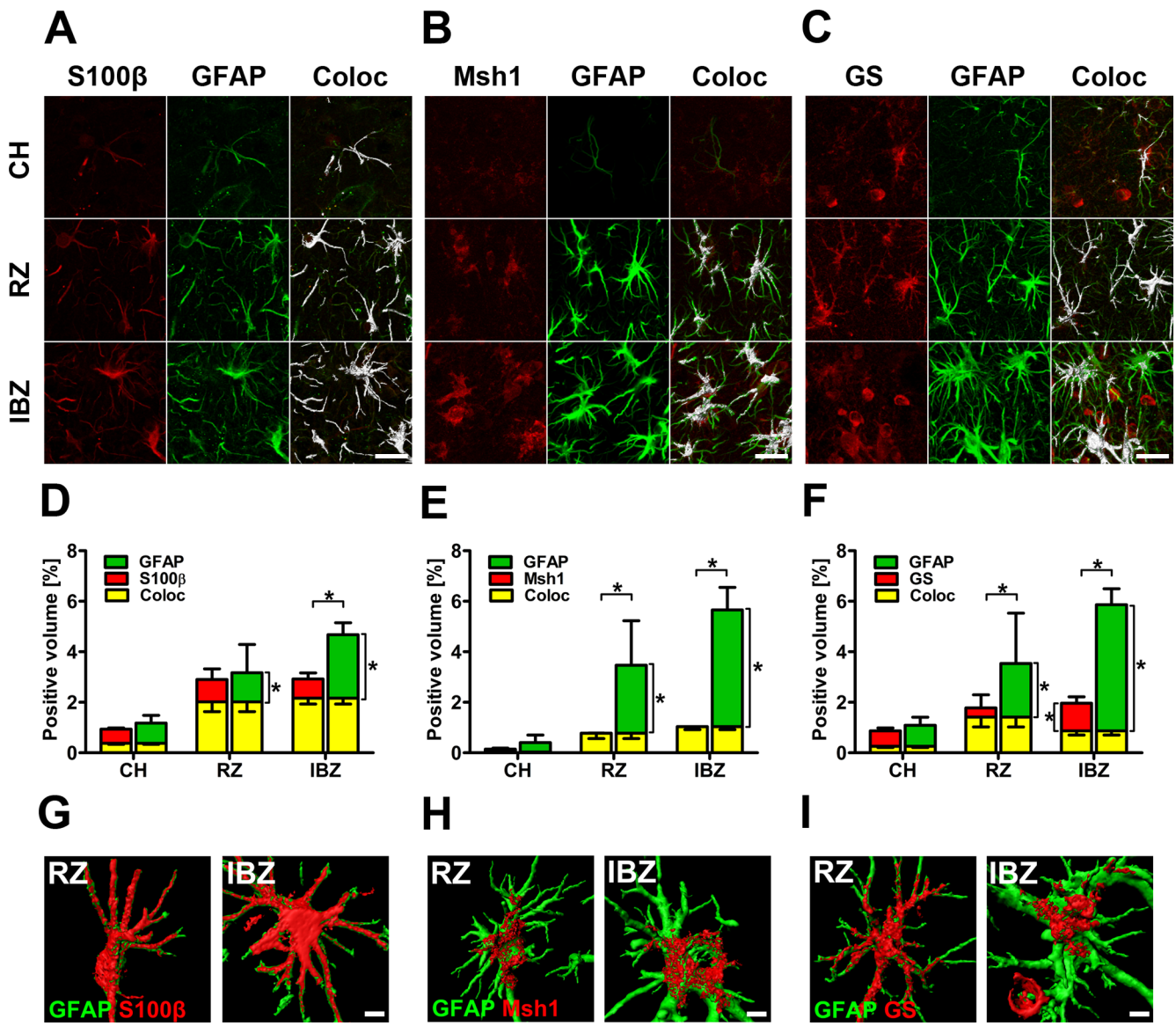

Fig. 2. Representative micrographs of colocalization of GFAP with (A) S100β, (B) Musashi1 (Msh1) and (C) glutamine synthetase (GS) within three defined regions of interest (CH: contralateral hemisphere, RZ: remote zone and IBZ: infarct border zone). Quantification of the volumes of (D) S100β, (E) Msh1, (F) GS as well as of GFAP and the according colocalized channel. (G–I) Exemplary illustration of rendered single astrocytes to visualize the degree of colocalization and the subcellular distribution of the markers. *P<0.05 by repeated measures one-way ANOVA for n=5. Scale bars are 20 µm (A–C) and 5 µm (G–I).

analyses and tested for normality at the level of P=0.05 by Shapiro-Wilk test. Within-subject comparisons of the three ROI were performed by multiple repeated measures (RM) one-way ANOVA with the volume of marker expression and colocalization, and the variables of the process analysis (volume, mean process diameter, mean process length and mean process branching) as dependent variables. Multiple testing was corrected by the Bonferroni method. The number of astrocytes within the remote and the infarct border zone was compared by *t*-test. All data were expressed as means ± standard deviation. *P*-values of less than 0.05 were considered statistically significant.

RESULTS

Colocalization of GFAP and other astrocyte markers

Expectedly and as a consequence of brain ischemia, we observed a marked increase of GFAP immunoreactivity within the ipsilateral hemisphere compared to the unaffected contralateral hemisphere (Figs 1 and 2A–C). The expression of S100β largely resembled that of GFAP except that S100β was additionally expressed in the nucleus and was not detected within the fine GFAP-positive process endings (Fig. 2A). Musashi1 (Msh1) was stained solely in the astrocyte soma proximal to the nucleus and at the basis of the large processes (Fig. 2B). Glutamine synthetase (GS) showed two different expression patterns: first, GS/GFAP double-positive cells and, second, ovoid GS-positive/GFAP-negative cells that occurred in the contralateral hemisphere and, to a larger extend, in the infarct border zone. With the exception of the latter population, we found the expression of S100β, Msh1 and GS always being concurrent with GFAP-positive cells and processes.

The quantitative analyses of marker expression and colocalization confirmed the visual impression that the GFAP immunoreactive volume significantly and progressively increased in the ipsilateral hemisphere compared to the contralateral hemisphere and furthermore in the infarct border zone compared to the remote zone (P<0.05 by RM one-way ANOVA). Interestingly, this increase was largely accompanied by colocalization with S100β in the remote zone, but not within the infarct border. Here, the fine processes were only positive for GFAP (Fig. 2D,G). Msh1 was hardly detectable within the control hemisphere and always

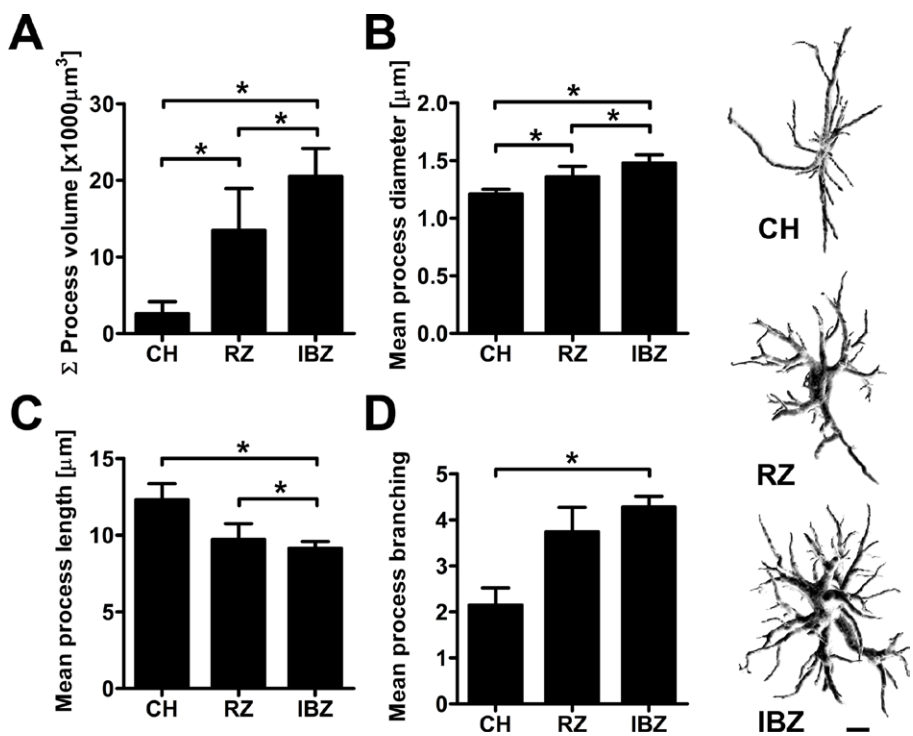

Fig. 3. Morphometric analysis of GFAP-positive astrocyte processes for the (A) summarized volume, (B) mean diameter, (C) mean length and (D) mean degree of branching. *P<0.05 by repeated measures one-way ANOVA for n=5. Scale bar is 10 µm.

colocalized with GFAP within the affected hemisphere (Fig. 2E). GS expression was rarely colocalized with GFAP within the control hemisphere, but the overlap was almost completely within the remote zone (Fig. 2F). Interestingly, the volume of colocalization of GS and GFAP decreased in the infarct border (Fig. 2F) as consequence of two different phenomena. At first, we observed a marked decrease of GS expression in single astrocytes, resulting in a rather peri-nuclear staining pattern (Fig. 2I). Moreover, the colocalized volume was further decreased by the above-mentioned GS single-positive cell population.

Morphological changes of GFAP-positive astrocyte processes

We found that among the markers applied, GFAP covered the largest volume of astrocytes. We hence used GFAP to further describe morphological astrocyte changes by quantifying process characteristics. In accordance with the visual impression and the determination of the GFAP-positive volume (see above), we observed a region-specific increase of the cumulated astrocyte process volume with smallest volumes in the contralateral hemisphere, moderate volumes in the remote zone, and largest ones in the infarct border zone (Fig. 3A). This was accompanied by an equivalent increase of the mean process diameter (Fig. 3B). In contrast, the mean length of astrocyte processes significantly decreased in the infarct border (9.2 ± 0.4 µm) when compared to the remote zone (9.7 ± 1 µm) or the contralateral hemisphere (12.3 ± 1 µm) (Fig. 3C). In the contralateral hemisphere, the astrocyte processes showed a mean branching level of 2.2 ± 0.4, which means that one leaving process ended on average in four terminal processes. In contrast, the branching level doubled in astrocytes within the infarct border zone (4.3 ± 0.3; average of 16 terminal processes, Fig. 3D), resulting in the typical bushy appearance of reactive astrocytes.

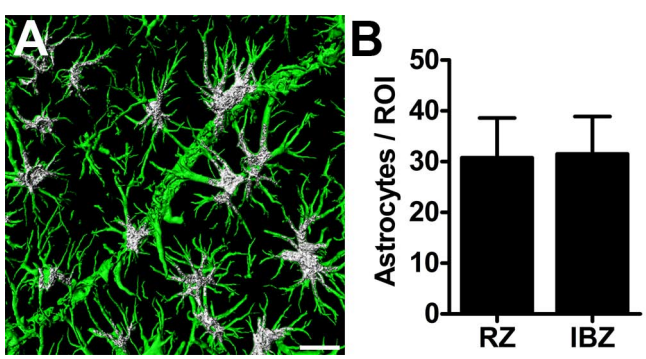

Fig. 4. (A) Illustration of GFAP positive astrocytes (green) and the colocalization between GFAP and Musashi1 (grey) within the peri-infarct area. (B) The quantification of GFAP/Musashi1 double-positive astrocytes within the remote zone (RZ) and the infarct border zone (IBZ). *n*=5. Scale bar is 20 µm.

Quantification of reactive astrogliosis

The identification of individual astrocytes was hardly possible within the infarct border zone as compared to the contralateral hemisphere and the remote zone. Here, the post-stroke astrogliosis was characterized by many interwoven processes which could not be definitely attributed to individual astrocytes. However, the rendered objects that resulted from the colocalization of GFAP and Msh1 (Fig. 4A) were suitable for individual cell quantification, since the colocalization of both markers solely occurred in the astrocytes' center. By applying this method, we found that the there was no numerical increase of astrocytes between the remote zone and the infarct border (Fig. 4B).

DISCUSSION

In this study, we investigated reactive astrogliosis following focal cerebral ischemia. We observed an activation pattern of GFAP-positive astrocytes being pathognomonic for focal lesions of the central nervous system. Moderately reacting astrocytes with conserved individual territories were found predominantly within the area remote from the lesion. In contrast, the border zone in direct vicinity to the lesion was characterized by strongly reacting astrocytes with interleaving processes and a disruption of individual domains, which is in agreement with previous studies (Sofroniew 2009). Of note, volume and arborisation of these processes increased depending on the proximity to the ischemic lesion. By further analyzing morphological changes, we could also demonstrate *in vivo* that an upregulation of GFAP primarily occurs in the processes of the astrocytes. An increased expression of the intermediary filament GFAP is a hallmark of astrogliosis and has nowadays become the prototypic marker for astrocytes. The observed GFAP upregulation particularly in the processes of astrocytes is in line with another study that used GFAP/eGFP transgenic mice to analyze volume changes of reactive astrocytes

ex vivo (Benesova et al. 2009). It is, however, also known from single-cell dye injection studies that GFAP stains only 15% of an individual astrocytes that, furthermore, in fact rather exhibits a bushy phenotype than a stellate one (Sun and Jakobs 2012). Hence, it remains unclear if the increase of GFAP-positive process volume is indeed a volume change of the astrocyte or an increased expression of intermediary filaments in the equally sized astrocyte. It seems, however, that GFAP, particularly in the processes, is important for the function of astrocytes, since Wilhelmsson and colleagues (2004) could demonstrate by performing single cell dye injection in transgenic mice lacking the intermediary filaments GFAP and vimentin that the territory addressed by a single astrocyte remained constant in the wild-types, whereas the hypertrophy of processes was significantly decreased in GFAP/Vimentin knockout animals.

The regional differences described above were also recapitulated by different expression profiles of proteins that were used as astrocyte markers (Wang and Walz 2003, Oki et al. 2010, Kim et al. 2012). Based on these findings, it is generally accepted that different astrocyte entities exist, and that different subclasses might be responsible for different functions that are either protective or detrimental with respect to the outcome after brain injury (Zamanian et al. 2012).

In this study, we introduced a novel object-based approach to quantify several characteristics of astrogliosis that may ultimately help to identify astrocyte subclasses. We established a protocol that allows us to quantify the degree of colocalization of two different astrocyte markers within the damaged brain. Standard procedures to assess colocalization such as the Pearson`s correlation coefficient (PCC) are highly sensitive for background noise, for high particle densities and are compromised by unequal distribution of fluorescence within the channels (Comeau et al. 2006). Those problems were solved by the Manders colocalization coefficients, but this method depends on the subjective determination of threshold values (Manders et al. 1992). Hence, Costes and colleagues (2004) suggested a statistical approach to determine the threshold automatically. However, we failed to apply this method to our confocal image stacks, most likely due to the high density of background particles. We therefore decided to calculate objects from the fluorescence and the colocalization channels and to exclude small objects according to the simple hypothesis that random background noise should give abundant signals, though which are small by volume. This method was feasible to quantify the colocalization of GFAP with other common astrocyte markers and ultimately allowed us to provide a more complete visualization of marker expression in reactive astrocytes. The approach is methodically simple to perform and can be applied using a variety of commercially available and open source imaging software packages.

Our investigation revealed that the calcium binding protein S100β was virtually always colocalized with GFAP-positive astrocytes, thus showing the highest degree of colocalization among the markers used. Differences between the respective marker (S100β and GFAP) and the colocalization volume can be explained both by exclusive nuclear expression of S100β and the more extensive expression of GFAP in fine processes, particularly in the peri-infarct area. As a consequence, we would recommend using GFAP for morphological analyses of processes, since it covers the broadest part of the astrocyte when using immunohistochemical markers.

Msh1 is a classical neural progenitor marker that is exclusively expressed in the neurogenic niches of the brain and in reactive astrocytes (Oki et al. 2010). We found detectable levels of Msh1 exclusively within the ipsilateral hemisphere. As for S100β, Msh1 was always colocalized with GFAP, with only marginal differences between the remote zone and the peri-infarct area. The exclusive peri-nuclear expression of Msh1 renders the protein an interesting candidate for cell counting, since staining provides non-overlapping objects even in regions with a dense astrocytic meshwork characterized by interwoven astrocyte processes. Surprisingly, we found no numerical differences of GFAP/Msh1-double-positive cells between the remote zone and the infarct border. This could either imply that proliferation occurred similar in the remote zone and the infarct border, or that no proliferation occurred. The latter hypothesis is supported by a study showing that only few astrocytes proliferate after stroke while a comparable amount underwents apoptosis. Hence, the overall number of astrocytes in the reactive zone remains nearly unchanged (Barreto et al. 2011).

Single cell gene expression analysis of primary astrocytes revealed that 94% of the cells expressed GS. GS was co-expressed with GFAP in 79% of the cases (Stahlberg et al. 2011). In line with this finding, we found that GS was

almost completely colocalized with GFAP in remote zone astrocytes. In contrast, we observed a significant decrease of colocalized volume in the peri-infarct area even though the volume of GS remained stable. This observation had two reasons: First, we observed numerous ovoid GS positive cells that were negative for GFAP. This cell population may comprise oligodendrocytes (Cammer 1990) and their progenitors (Baas et al. 1998). The obvious increase of this cell population can be explained by the fact that oligodendrocyte precursors rapidly increase numerically in the peri-infarct area by migration and proliferation on site to ultimately replenish the mature oligodendrocyte cell pool and to remyelinate the affected brain tissue (Tanaka et al. 2003). Second, we showed that astrocytic GS expression decreased from the remote zone to the infarct border zone (Fig. 2I). Downregulation of glutamine synthetase in pathological conditions have been previously described *in vitro*: after scratch wound, GS was downregulated in astrocytes close to the injury. Moreover, siRNA-mediated GS knockdown significantly increased the migratory capacity of affected astrocytes (Zou et al. 2011). Hence, we could clearly identify two different astrocyte subclasses occurring after stroke, being discriminable by their GS expression level which might also determine their migratory capacity.

CONCLUSIONS

We found both S100β and Msh1 in colocalization with GFAP-positive astrocytes albeit the cellular compartments of expression differed. Among the markers used, GFAP stained the most astrocyte processes and is hence suitable for the analysis of qualitative characteristics of astrogliosis. Due to its peri-nuclear localization, Msh1 is appropriate to estimate the total number of astrocytes even in regions with severe reactive astrogliosis. GS expression in GFAP-positive astrocytes was high in the remote zone and low at the infarct border, probably indicating two astrocyte subclasses with may be characterized by different migratory capacities. The increase of GFAP-positive volume between the remote zone and the peri-infarct area was not caused by a numerical increase of astrocytes, but by an increased volume and arborisation of GFAP-positive processes. These findings further emphasize the concept of moderately and strongly reacting astrocytes in remote and adjacent areas of focal brain injuries, respectively, and may help to further characterize and understand the pathophysiological mechanisms of astrogliosis in order to ultimately identify specific therapeutic targets.

REFERENCES

Baas D, Dalencon D, Fressinaud C, Vitkovic L, Sarlieve LL (1998) Oligodendrocyte-type-2 astrocyte (O-2A) progenitor cells express glutamine synthetase: Developmental and cell type-specific regulation. Mol Psychiatry 3: 356–361.

Barreto GE, Sun X, Xu L, Giffard RG (2011) Astrocyte proliferation following stroke in the mouse depends on distance from the infarct. PLoS One 6: e27881.

Benesova J, Hock M, Butenko O, Prajerova I, Anderova M, Chvatal A (2009) Quantification of astrocyte volume changes during ischemia in situ reveals two populations of astrocytes in the cortex of GFAP/EGFP mice. J Neurosci Res 87: 96–111.

Bolte S, Cordelieres FP (2006) A Guided tour into subcellular colocalization analysis in light microscopy. J Microsc 224: 213–232.

Cammer W (1990) Glutamine synthetase in the central nervous system is not confined to astrocytes. J Neuroimmunol 26: 173–178.

Comeau JW, Costantino S, Wiseman PW (2006) A guide to accurate fluorescence microscopy colocalization measurements. Biophys J 91: 4611–4622.

Costes SV, Daelemans D, Cho EH, Dobbin Z, Pavlakis G, Lockett S (2004) Automatic and quantitative measurement of protein-protein colocalization in live cells. Biophys J 86: 3993–4003.

Kim WR, Kim JY, Moon Y, Kim HJ, Kim H, Sun W (2012) Regional difference of reactive astrogliosis following traumatic brain injury revealed by HGFAP-GFP transgenic mice. Neurosci Lett 513: 155–159.

Kimelberg HK (2004) The problem of astrocyte identity. Neurochem Int 45: 191–202.

Liberto CM, Albrecht PJ, Herx LM, Yong VW, Levison SW (2004) Pro-regenerative properties of cytokine-activated astrocytes. J Neurochem 89: 1092–1100.

Manders EM, Stap J, Brakenhoff GJ, van DR, Aten JA (1992) Dynamics of three-dimensional replication patterns during the S-phase, analysed by double labelling of DNA and confocal microscopy. J Cell Sci 103: 857–862.

Menet V, Prieto M, Privat A, Ribotta M (2003) Axonal plasticity and functional recovery after spinal cord injury in mice deficient in both glial fibrillary acidic protein and vimentin genes. Proc Natl Acad Sci U S A 100: 8999–9004.

Okada S, Nakamura M, Katoh H, Miyao T, Shimazaki T, Ishii K, Yamane J, Yoshimura A, Iwamoto Y, Toyama Y, Okano H (2006) Conditional ablation of stat3 or socs3 discloses a dual role for reactive astrocytes after spinal cord injury. Nat Med 12: 829–834.

Oki K, Kaneko N, Kanki H, Imai T, Suzuki N, Sawamoto K, Okano H (2010) Musashi1 as a marker of reactive astrocytes after transient focal brain ischemia. Neurosci Res 66: 390–395.

Paxinos G, Watson C (2006) The Rat Brain in Stereotaxic Coordinates (6th ed). Academic Press, New York, NY.

Popa-Wagner A, Buga AM, Kokaia Z (2011) Perturbed cellular response to brain injury during aging. Ageing Res Rev 10: 71–79.

Riegelsberger UM, Deten A, Posel C, Zille M, Kranz A, Boltze J, Wagner DC (2011) Intravenous human umbilical cord blood transplantation for stroke: impact on infarct volume and caspase-3-dependent cell death in spontaneously hypertensive rats. Exp Neurol 227: 218–223.

Shimada IS, Borders A, Aronshtam A, Spees JL (2011) Proliferating reactive astrocytes are regulated by Notch-1 in the peri-infarct area after stroke. Stroke 42: 3231–3237.

Silver J, Miller JH (2004) Regeneration beyond the glial scar. Nat Rev Neurosci 5: 146–156.

Singan VR, Jones TR, Curran KM, Simpson JC (2011) Dual channel rank-based intensity weighting for quantitative co-localization of microscopy images. BMC Bioinformatics 12: 407.

Sofroniew MV (2009) Molecular dissection of reactive astrogliosis and glial scar formation. Trends Neurosci 32: 638–647.

Sofroniew MV, Vinters HV (2010) Astrocytes: Biology and pathology. Acta Neuropathol 119: 7–35.

Stahlberg A, Andersson D, Aurelius J, Faiz M, Pekna M, Kubista M, Pekny M (2011) Defining Cell populations with single-cell gene expression profiling: Correlations and identification of astrocyte subpopulations. Nucleic Acids Res 39: e24.

Sun D, Jakobs TC (2012) Structural remodeling of astrocytes in the injured CNS. Neuroscientist 18: 567–588.

Takahashi H, Matsumoto H, Kumon Y, Ohnishi T, Freeman C, Imai Y, Tanaka J (2007) Expression of heparanase in nestin-positive reactive astrocytes in ischemic lesions of rat brain after transient middle cerebral artery occlusion. Neurosci Lett 417: 250–254.

Tanaka K, Nogawa S, Suzuki S, Dembo T, Kosakai A (2003) Upregulation of oligodendrocyte progenitor cells associated with restoration of mature oligodendrocytes and myelination in peri-infarct area in the rat brain. Brain Res 989: 172–179.

Walz W (2000) Controversy surrounding the existence of discrete functional classes of astrocytes in adult gray matter. Glia 31: 95–103.

Wang K, Walz W (2003) Unusual topographical pattern of proximal astrogliosis around a cortical devascularizing lesion. J Neurosci Res 73: 497–506.

Wang K, Bekar LK, Furber K, Walz W (2004) Vimentin-expressing proximal reactive astrocytes correlate with migration rather than proliferation following focal brain injury. Brain Res 1024: 193–202.

White RE, McTigue DM, Jakeman LB (2010) Regional heterogeneity in astrocyte responses following contusive spinal cord injury in mice. J Comp Neurol 518: 1370–1390.

Wilhelmsson U, Li L, Pekna M, Berthold CH, Blom S, Eliasson C, Renner O, Bushong E, Ellisman M, Morgan TE, Pekny M (2004) Absence of glial fibrillary acidic protein and vimentin prevents hypertrophy of astrocytic processes and improves post-traumatic regeneration. J Neurosci 24: 5016–5021.

Wilhelmsson U, Bushong EA, Price DL, Smarr BL, Phung V, Terada M, Ellisman MH, Pekny M (2006) Redefining the concept of reactive astrocytes as cells that remain within their unique domains upon reaction to injury. Proc Natl Acad Sci U S A 103: 17513–17518.

Zamanian JL, Xu L, Foo LC, Nouri N, Zhou L, Giffard RG, Barres BA (2012) Genomic analysis of reactive astrogliosis. J Neurosci 32: 6391–6410.

Zou J, Wang YX, Mu HJ, Xiang J, Wu W, Zhang B, Xie P (2011) Down-regulation of glutamine synthetase enhances migration of rat astrocytes after in vitro injury. Neurochem Int 58: 404–413.